Regenspurg, S., Schild, D., Schäfer, T., Huber, F., Malmström, M. E. (2009): Removal of uranium(VI) from the aqueous phase by iron(II) minerals in presence of bicarbonate. - Applied Geochemistry, 24, 9, 1617-1625

DOI: 10.1016/j.apgeochem.2009.04.029

Title

Removal of uranium(VI) from the aqueous phase by iron(II) minerals in presence of bicarbonate

Authors

Simona Regenspurg[1,2], Dieter Schild[3], Thorsten Schäfer[3], Florian Huber[3], Maria E. Malmström[2]

Affiliations

[1] current address: EPFL ENAC ISTE-GE, Station 6, 1015 Lausanne, Switzerland

simona.regenspurg@epfl.ch

Fax: + 41 21 693 6205

[2] Industrial Ecology, Royal Institute of Technology (KTH), SE-10044 Stockholm, Sweden

[3] Institut für Nukleare Entsorgung (INE), Forschungszentrum Karlsruhe, 76344 Eggenstein-Leopoldshafen, Germany

Abstract

Uranium(VI) mobility in groundwater is strongly affected by sorption of mobile U(VI) species (e.g. uranyl, UO_2^{2+}) to mineral surfaces, precipitation of U(VI) compounds, such as schoepite $(UO_2)_4O(OH)_6 * 6H_2O$), and by reduction to U(IV), forming sparingly soluble phases (uraninite; UO_2). Especially the latter pathway would be very efficient for long-term immobilization of uranium. In nature, ferrous iron is an important reducing agent for U(VI) because it frequently occurs either dissolved in natural waters, sorbed to matrix minerals, or structurally bound in many minerals. Redox reactions between U(VI) and Fe(II) depend not only on the availability of Fe(II) in the environment, but also on the chemical conditions in the aqueous solution. Under natural groundwater condition U(VI) forms complexes with many anionic ligands, which strongly affect its speciation. Especially carbonate is known to form stable complexes with uranium, rising the question if U(VI), when complexed by carbonate, can be reduced to UO_2. The goal of this study was to find out if Fe(II) when structurally bound in a mineral (as magnetite, Fe_3O_4) or sorbed to a mineral surface (as corundum, Al_2O_3) can reduce U(VI) to U(IV) in presence of bicarbonate. Batch experiments were conducted under anaerobic conditions to observe uranium removal from the aqueous phase by the two minerals in dependence of bicarbonate addition (1 mM), uranium concentration (0.01-30 μM) and pH value (6-10). Immediately after the experiments, the mineral surfaces were analyzed by X-ray photoelectron spectroscopy (XPS) to obtain information on the redox state of uranium bound to the solid surfaces. XPS results gave evidence that U(VI) can be reduced both by magnetite and by corundum amended with Fe(II). In presence of bicarbonate the amount of reduced uranium on the mineral surfaces increased compared to carbonate-free

46 solutions. This can be explained by the formation of Fe(II) carbonates on the mineral
47 surfaces which represent an easily available Fe(II) pool for the U(VI) reduction. We also
48 consider a facilitated U(VI) reduction as possible when uranium is present as a carbonate
49 complex compared to non-complexed uranium (e.g. uranyl).
50
51
52
53 **Keywords**
54 uranium, iron, iron minerals, magnetite, corundum, siderite, bicarbonate, reduction, XPS,
55 uraninite, uranyl, sorption, surface precipitation
56

Main text

Introduction

Uranium is a naturally occurring element that can be found in low levels within many rocks, sediments and soils. Due to its radioactivity and toxicity (carcinogenic for humans), uranium is a hazardous contaminant in the environment and the World Health Organization (WHO) recommends a drinking water limit of 0.015 mg/L (WHO, 2004). The average uranium concentration in the earth crust is between 2 and 4 ppm, but it can be enriched in soil and groundwater by several anthropogenic activities, such as by the release from mill tailings of uranium mines, as a consequence of the use of depleted uranium for military devices (DU ammunition), or by agricultural application of phosphate fertilizers, which are often associated with uranium. The main use of uranium is as fuel in nuclear power plants and thus, it is a primary component of spent nuclear fuel and high level nuclear waste. Consequently it is of high concern for nuclear waste management. A thoroughly understanding of the interactions of uranium with geological materials and its behavior in groundwater is of high relevance both for remediation strategies of contaminated sites and for the safety of final nuclear waste repositories.

Uranium mobility in groundwater is controlled by its redox, sorption and complexation behavior. At oxic conditions, it occurs predominantly in the redox state of +VI (UO_2^{2+} or uranyl). A removal of uranium from the aqueous phase is possible by sorption to solid surfaces, precipitation as U(VI) mineral, such as schoepite ($(UO_2)_4O(OH)_6*6H_2O$ or $UO_2(OH)_2*H_2O$), coffinite ($U(SiO_4)_{1-x}(OH)_{4x}$), autunite ($Ca(UO_2)_2(PO_4)_2*10\text{-}12H_2O$) or sodium uranate $Na_2O(UO_3)_2.6H_2O$), or by reduction to U(IV) forming hardly soluble solid phases such as UO_2 (uraninite), U_3O_8, UO_{2+x}. Dissolved in natural water, aqueous

uranium is prone to complexation with phosphate, silicate, sulfate, fluoride and especially with carbonate (Langmuir, 1978). Consequently, more than 42 dissolved uranium species, 89 uranium minerals and 368 inorganic crystal structures that contain U(VI) are known to date (Langmuir, 1978; Burns, 2005). Especially bicarbonate (HCO_3^-) forms strong aqueous uranium-carbonate complexes (UO_2CO_3, $UO_2(CO_3)_2^{2-}$ and $UO_2(CO_3)_3^{4-}$) and, thus, in the presence of carbonate or bicarbonate in water U(VI) is highly mobile (e.g. Grenthe et al., 1984; Nguyentrung et al., 1992; Baborowski and Bozau, 2006).

Reduction of mobile U(VI) to sparingly soluble UO_2 can be induced for example by Fe(II) or sulphide - a process which is possible in the aqueous phase (Privalov et al., 2003), but enhanced in the presence of solid surfaces acting as catalysts (Jeon et al., 2005). Accordingly, it has been shown that sulphide- or Fe(II) bearing minerals like pyrite (FeS_2), magnetite (Fe_3O_4), or biotite ($K(Mg, Fe)_3AlSi_3O_{10}(F, OH)_2$) can reduce U(VI) (e.g. Wersin et al., 1994; Scott et al., 2005; Ilton et al., 2004, 2006). Iron in the redox state of +II is an ubiquitous compound in all natural systems, occurring dissolved in water, structurally bound in many minerals and sorbed to mineral surfaces. The effect of Fe(II) containing minerals on the long term reduction of U(VI) is of high importance, due to the omnipresence of these minerals in the earth crust. Especially for the construction of deep ground repositories for radioactive waste the interactions of radionuclides with the minerals in the backfill and in the surrounding bedrock have to be considered. For example, in Sweden the nuclear waste will potentially be stored in a repository hosted in the granitic rock. The groundwater circulating in these granitic aquifers, which might react one day with the nuclear waste, contains, besides NaCl (ca. 10 mM) high concentration of $NaHCO_3$ (ca. 1 mM; Metz et al., 2003). Granite contains

several Fe(II) minerals, such as pyrite, biotite or magnetite, which are responsible for an average FeO content in granite of 1.68 wt.-% (Blatt and Tracy, 1996). Previous studies indicated that Fe(II) in all of the three minerals can reduce U(VI) to U (IV) (Wersin et al., 1994; Ilton et al., 2004; Scott et al., 2005) but none of these studies considered the influence of bicarbonate on the reduction. As mentioned above, carbonate is known to form very stable aqueous complexes with U(VI), a fact which is often used to prevent U(VI) mineral precipitation in experiments (Payne et al., 2002) or to extract uranium from soil (Zhou and Gu, 2005). However, U(VI) carbonate complexes are also known to sorb to mineral surfaces, thereby forming ternary surface complexes with Fe(III) as has been shown by infrared spectroscopy (Ho and Miller,1986) and X-ray absorption spectroscopy on the hematite surface (Bargar et al., 2000). Up to date, there are only few studies on the potential reduction of U(VI) by Fe(II) in the presence of (bi)carbonate in the scientific literature (e.g. Behrends and van Kappellen, 2005). To the best of our knowledge, in none of them were spectroscopic methods applied to verify uranium reduction. The main goal of our study was to find out if U(VI), i.e. UO_2^{2+} can be reduced by Fe(II) which is either structurally bound in Fe(II) containing minerals or sorbed to a mineral surface. Moreover, we aimed at finding out to what extent HCO_3^- and the pH value affects this process. The experimental conditions in solution were held near to natural groundwater conditions.

Materials and Method

Magnetite (Fe_3O_4) was prepared by reaction of 0.3 M $FeSO_4$ with 3.33 M KOH and 0.27 M KNO_3 (Cornell and Schwertmann, 1996). The mineral suspension was dialyzed

126 against deionised water which was changed on a daily basis in a Ar-atmosphere in a
127 glove box until the electric conductivity was stable and below 10 µS/cm over 24 hours.
128 Mineral composition was verified to consist solely out of magnetite by powder X-ray
129 diffraction. XRD patterns were recorded from 5 to 80° 2θ, using 0.01° 2θ steps, and a 2 s
130 counting time per step with a Bruker AXS D8 powder diffractometer equipped with a
131 BSI (Baltic Scientific Instrument) Si(Li) solid detector, and CuKα radiation. Surface area
132 of magnetite was determined by the BET method (5 step nitrogen sorption of 0.08 g
133 samples) in two replicates. Suspensions of 2 g/L magnetite with a specific surface area of
134 19.7 m^2/g were used for the experiments. A synthetic corundum (α-Al_2O_3) suspension
135 (Krahn; purity > 99.99 %; particle size: 0.2 µm; surface area: 14.5 m^2/g; specifications
136 from the manufacturer) was diluted with MilliQ-water to obtain a final amount of 2 g/L α
137 -Al_2O_3. The ionic strength was set to 0.01 M by adding NaCl to all mineral suspensions.
138 Different chemical conditions were obtained by addition of $NaHCO_3$ (0 or 0.001 M) or
139 $FeCl_2$ (0 or 0.001 M). Finally, the pH values were adjusted to 6, 8, or 10 (pH measured
140 with a combined glass electrode) by addition of HCl and NaOH (Table 1). All solutions
141 were purged 1 h with nitrogen gas before addition to the suspensions in an anaerobic
142 glove box. Therein, samples were kept at room temperature during the experiment and
143 anoxic conditions were assured.
144 Experiments were performed in polyethylene (PE) bottles containing 20 mL of
145 suspension. The used chemicals (pro analysi) and gas (> 99.999 %) were of high purity.
146 After 24 h, uranium was added from a stock solution of $UO_2(NO_3)_2$ to the mineral
147 suspensions to get final uranium concentrations between $3*10^{-7}$ M and $3*10^{-5}$ M. The pH
148 was re-adjusted (6, 8, 10) immediately and again after 7 and 13 days. Table 1 gives an

overview of all samples used in this batch. After a reaction time of 27 days, pH and redox potential (measured with a platinum electrode and Ag/AgCl reference electrode) were measured. Three mL of all suspensions kept originally at pH 6 or 10 were ultra-centrifuged (90,000 rpm) to separate the dissolved Fe and U species from colloidal compounds. To prevent sample oxidation during centrifugation (outside the glovebox), samples were transferred in air-tight sealed PE centrifuge tubes. After centrifugation, the tubes were transferred back into the glove box. From the samples kept originally at pH 8 (the highest U concentration), only 0.5 mL were removed from the suspensions and filtered (0.22 µm). The pH in the remaining suspensions was adjusted to four by addition of HCl. The applied acid was degassed and stored already since several month in the permanently Ar filled glovebox equipped with a gas purification system. After another 48 h, 3 mL of these acidified samples were again ultra-centrifuged (90,000 rpm) in air-tight tubes and separated from the solids. In all supernatants and filtrates, the pH-value was measured and the elemental composition was determined by inductive coupled plasma mass-spectrometry (ICP-MS), which has a detection limit for U of 0.006 µg/L and for Fe of 0.2 µg/L. It was assumed that uranium in the aqueous phase exists predominantly in the redox state of +VI, because U(IV) would form solid precipitates (UO_2).

Theoretical uranium speciation and complexation in the different solutions were calculated with the HYDRA/ MEDUSA software using the program internal database complex.db and complex.elb (Puigdomenech, 2004).

XPS analysis

After separation from the supernatant, selected samples of the solids were prepared in the glove box at inert gas (Ar) condition for X-ray photoelectron spectroscopy (XPS) analysis. Portions of powder samples, dried at room temperature, were pressed onto indium foil and mounted on the sample holder. By means of an O-ring sealed vacuum transfer vessel (PHI model 04-110) samples were transported from inside the glovebox into the XPS instrument without air-contact. Within the following two days, samples were analyzed using a Physical Electronics Inc. (PHI) model 5600ci spectrometer equipped with Mg K_α, Al K_α, and monochromatic Al K_α X-ray sources. Electrons passing the spherical capacitor analyzer were detected by a 16-channel detector. Charging of isolating sample surfaces, due to emitting photo- and Auger electrons was compensated by a low-energy electron flood gun in case of monochromatic X-ray excitation.

Elemental lines of pure metals (Mg K_α: Cu $2p_{3/2}$ at 932.62 eV, Ag $3d_{5/2}$ at 368.22 eV, Au $4f_{7/2}$ at 83.95 eV) with well-established binding energies were used to calibrate the binding energy scale of the spectrometer following Seah et al. (1998). Subsequently, these elemental lines were also measured by Al K_α and monochromatic Al K_α X-ray excitation. The determined standard deviation of binding energies were within ± 0.1 eV for conductors and within ±0.2 eV for non-conducting samples. A linear regression between reference data and measured values of the calibration was used to correct measured binding energies of samples.

Survey scans were recorded first by monochromatic Al K_α excitation, source power maximal 200 W, to identify the elements and to determine their atomic concentrations at the sample surfaces. An area of about 1 mm in diameter was excited by the monochromatic Al K_α X-rays. Samples prepared had sizes of about 5 mm in diameter

allowing multiple analyses at previously non-irradiated areas. Data analysis and curve fitting were performed using the PHI Multipak program. Narrow scans of the elemental lines were measured at 23.5 eV pass energy of the hemispherical analyzer. Elemental lines at the surface of magnetite showed a small shift due to charging relative to the conducting magnetite bulk, presumably due to formation of some isolating hydroxide at the surface. Therefore, U 4f lines in magnetite as well as in all (isolating) corundum samples were charge referenced to the C 1s line of adventitious hydrocarbon (C_xH_y) at 284.8 eV. Solely for the elemental lines of Fe 2p and O 1s charge reference occurred at the O 1s binding energy reference of bulk Fe_3O_4 at 530.0 eV.

Potential beam induced U(VI) reduction during XPS measurement was considered by recording narrow scans of the U 4f elemental line of the samples by monochromatic Al K_α X-rays in combination with an electron flood gun as well as with the Al-K_α standard source equipped with an aluminum window. Besides different overall charging due to the different X-ray sources, the spectra of the elemental lines were similar and explicitly no further change at the U4f lines were observed during the measurement. Consequently, beam reduction of U(VI) can be considered as insignificant for our experiments.

With monochromatic Al K_α X-ray excitation, bremsstrahlung induced background intensity and X-ray satellites are absent, yielding a detection limit for uranium of about 0.02 at-%. Moreover, thermal impact to the sample from the monochromatic X-ray source is prevented.

3. Results and discussion

3.1. Uranium immobilization – quantitative analysis

In all experimental mineral suspensions, uranium had been strongly removed from the aqueous solutions (58 to 99 % of the initial uranium concentration) after 27 days (Table 1). For removal mechanisms, we consider surface sorption of U(VI), precipitation of solid U(VI) phases and reduction and precipitation of U(IV) phases. Additionally, the release of Fe from the minerals and precipitation of new iron phases as Fe(II)- and Fe(III)-hydroxides or Fe(II)-carbonate and the sorption of uranium to these new surfaces will be discussed. Results indicated that uranium removal from solution depends on the uranium concentration, the pH-value, the presence of bicarbonate and the Fe(II) availability, i.e. the Fe(II) source. These factors will be discussed in the following sections.

3.1.1. Effect of initial uranium concentration

Conditions of oversaturation of the aqueous phase with respect to solid uranium (VI) compounds are easily established under experimental, carbonate-free suspensions. To determine differences between the uranium uptake from the aqueous phase in over- and unsaturated solutions, the initial uranium concentration was varied in the magnetite suspensions (pH 6, 8 and 10) to receive final values of $2.9 * 10^{-5}$, $8.9 * 10^{-6}$ and $9.9 * 10^{-8}$ M (Table 1). Initial and final uranium concentrations were plotted into a predominance diagram (Figure 1a), which indicates that the predominant uranium species at higher uranium concentrations are the U(VI) minerals schoepite $UO_2(OH)_2 * H_2O$ and sodium uranate ($Na_2O_7(UO_3)_2$). This observation implies that precipitation of solid phases for the two higher concentrated uranium suspensions must be considered. Only for the lowest initial uranium concentration ($9.9 * 10^{-8}$ M), the aqueous phase is unsaturated with respect

240 to uranium containing solids, which implies that uranium can only be removed by
241 sorption of U(VI) or reduction and precipitation as U(IV) species in these cases.
242 Nevertheless, we worked in most of our experimental suspensions with the highest
243 uranium concentration (2.95 *10^{-5} M), because the strong removal of uranium resulted in
244 uranium concentrations close to the detection limit of ICP-MS. Also, XPS measurements
245 require a relatively high uranium concentration on the mineral surfaces (0.02 atomic- %)
246 to be detected and evaluated properly. Although we never observed experimental
247 evidence for the formation of schoepite or sodium uranate, their possible precipitation
248 and its effect of providing new surface sites for sorption needs to be considered in the
249 obtained results.
250
251 **3.1.2. Effect of pH values and redox conditions**
252 Table 1 shows the pH values adjusted in the beginning and measured at the end of the
253 experiment as well as the measured final redox potentials (Eh) in all experimental
254 suspensions. Although the pH was re-adjusted to initial pH (6, 8, 10) twice during the
255 experiments, a strong shift to higher values was observed at the end (Table 1). As the
256 most probable reactions responsible for this pH increase we consider a slow surface
257 protonation and possibly (at lower pH) mineral dissolution.
258 Measured Eh data of all samples were between -84 and -416 mV and increased to
259 negative values with increasing pH. Figure 2a shows the measured pH-, Eh data plotted
260 in an Eh/pH stability diagram together with the redox equilibrium lines of the stability
261 area of an Fe(II)/ Fe(III) buffer, which was constructed using data from Felmy et al.
262 (1989) and Rai et al. (2002), who worked with iron powder. Thus, the lower line was

obtained by the equation pe + pH = 2 (Felmy et al., 1989) and the upper line by pe + pH = 4 (Rai et al., 2002). All samples appear to be in equilibrium with the Fe(II)/Fe(III) couple - including the three corundum suspensions that have not been added iron. Measured iron concentrations of these Al_2O_3-solutions revealed an iron concentration of 3-6 µg/L (=5-10*10^{-8} M), which indicates some Fe-contamination of the corundum samples. According to manufacturer information, the iron content in the corundum is below 20 ppm, corresponding to a maximum of 40 µg/L in each of our experimental suspensions (if corundum would be completely dissolved). Thus, the apparent equilibrium with the Fe(II)/Fe(III) can be explained if both redox states of iron are present in the corundum contamination or if initially Fe(III) was reduced by U(VI). A similar observation, as found in our study for the uranium system, was described for reductive dissolution of PuO_2 which is also strongly controlled by the Fe(II)/Fe(III) redox couple (Rai et al., 2002). The diagram 2a further indicates that at the present pH and redox conditions as well as when considering the Fe concentration in solution (given as 10 µM in the calculations), the solutions are oversaturated with respect to the formation of magnetite and hematite (Fe_2O_3). The measured total iron concentration in the solutions is considered to be predominantly in the redox state +II, because at the given pH conditions (> 3.5), the Fe(III), which potentially had formed by reduction of U(VI) would predominantly precipitate as Fe(III) hydroxide/-oxide. The Fe(II) concentration in the magnetite suspensions usually increased with increasing pH (except in bicarbonate containing solutions, where siderite precipitation can be expected; Fig. 2b) and is between 1 *10^{-5} M and 2*10^{-4} M (Table 1). In contrast to magnetite, the amount of

285 dissolved Fe(II) decreased with increasing pH in Fe(II) amended corundum suspensions
286 both, in presence and absence of bicarbonate.
287 In general, with increasing pH and increasing negative Eh, less uranium was removed
288 from the aqueous solutions (Table 1). As shown in the two predominance diagrams of
289 U(VI) in Fig. 1a and b, at higher pH values (> 7) negatively charged complexes (e.g. of
290 $UO_2(OH)_3^-$ or $UO_2(CO_3)_2^{2-}$) are predominant in the aqueous phase. Therefore, less
291 uranium sorption to negatively charged surfaces of oxide minerals can be expected (the
292 point of zero charge (pH_{pzc}) of Al_2O_3 is 6.8-7.2; Mustafa et al., 1998 and of Fe_3O_4 is 6.4-
293 7.1; Cornell and Schwertmann, 1996). Clearly, the lowest U removal from solution (58
294 %) occurred for magnetite in presence of bicarbonate at an initial pH of 10 (Table 1). We
295 explain this observation with the competition of uranium complexes (e.g. $UO_2(OH)_3^-$)
296 with carbonate for sorption sites on the negatively charged mineral surface.
297

298 **Acidification to pH 4**

299 After 27 days, mineral suspensions initially adjusted to pH 8 were acidified to pH 4. It
300 was expected that at this pH, sorbed U(VI) and surface precipitates of uranium, e.g.
301 schoepite ($UO_2(OH)_2*H_2O$), would desorb and dissolve, respectively, and only the
302 sparingly soluble, reduced form of uranium, i.e. UO_2, would remain dominantly in the
303 solid phase. Figure 3 compares the uranium concentrations measured in different
304 suspensions before and after acidification. In case of Fe(II)-free corundum only about 60
305 % of previously bound uranium were released to the aqueous phase (Table 1), indicating
306 that a part of the formed surface precipitates or sorbed U(VI) species are quite stable
307 against acidification because no, or only little uranium reduction (due to Fe(II)

308 contamination) can be expected in these suspensions. The release of uranium in the Fe(II)
309 amended corundum suspension was significantly lower (35 % of previously bound
310 uranium), indicating that a considerable amount of uranium might have been reduced to
311 less soluble UO_2. In case of magnetite suspensions, only a relatively small fraction of pH
312 8 surface accumulated uranium was released by acidification to pH 4 (9.5 %; Figure 3)
313 indicating that also Fe(II) within magnetite reduced partially the U(VI) to sparingly
314 soluble U(IV). However, due to oxidation of Fe(II) to Fe(III) and probable subsequent
315 precipitation of Fe-hydroxide (Figure 2a), sorption or co-precipitation of U(VI) on these
316 oxides can not be excluded as an additional or alternative pathway for removal of U from
317 the aqueous solution (Duff et al., 2002). However, uranium associated with Fe(III) phases
318 are unlikely to remain sorbed at the positively charged Fe(III)-hydroxide surfaces at low
319 pH where the positively charged uranyl (UO_2^{2+}) dominates the aqueous speciation
320 (Missana et al., 2003), which is inconsistent with the observed low degree of U release
321 upon acidification.
322 Although we expected at pH 4 no change of the Fe(II)/Fe(III) redox equilibrium (Rovira
323 et al., 2007), a strong increase in the Fe(II) concentration was observed due to
324 acidification (from $2.2*10^{-5}$ M - $9.4*10^{-6}$ M at pH 8-9 (Table 1) to $7.8*10^{-5}$ - $9.5*10^{-5}$
325 M at pH 4 (Table 2)). Clearly, the used synthetic magnetite is more reactive as compared
326 to commercial available magnetite (Rovira et al., 2007) which implicates either a
327 desorption of adsorbed Fe(II) or dissolution of weakly crystalline iron species bound to
328 the magnetite surface. Especially in the bicarbonate suspensions the release of iron at low
329 pH values was very high, indicating dissolution of previously formed siderite ($FeCO_3$).

330 Simultaneously, uranium concentration increased in this solution which is a consequence
331 of desorption of siderite-surface bound uranium during siderite dissolution (Fig. 3).
332
333 **3.1.3 Effect of bicarbonate**
334 Comparison of the predominance diagrams in Figure 1a and 1b shows the strong effect of
335 carbonate on uranium speciation in the aqueous solution. Instead of positively charged
336 uranyl (UO_2^{2+}) species, which are dominating under CO_2-free conditions, the solutions in
337 presence of carbonate contain predominantly negatively charged $UO_2(CO_3)_2^{2-}$, or
338 uncharged UO_2CO_3 complexes, with different sorption properties. Uranium concentration
339 measured in this study in presence and absence of bicarbonate followed this behavior: In
340 general, more uranium was found in the aqueous solution in presence of bicarbonate
341 (Table1). The concentration of uranium remaining in the aqueous solution also increased
342 with increasing pH ($\geq$ 8) (Figure 4). This is consistent with the formation of (aqueous)
343 uranium carbonate complexes which sorb less than carbonate-free uranium species.
344 Another effect of bicarbonate addition at pH $\geq$ 8 was a decrease in the aqueous Fe(II)
345 concentration in both magnetite and corundum suspensions, which can be explained by
346 the formation of $FeCO_3$ precipitates (Fig. 2b) removing the Fe(II) from the aqueous
347 phase. Acidification to pH 4 mobilized the iron again which is either due to desorption of
348 surface bound Fe(II) or dissolution of siderite or Fe(III)hydroxides, formed by reduction
349 of U(VI).
350
351 **3.1.4 Effect of Fe(II) source**

352 One of the central questions in this study was to find out whether the structural bound
353 Fe(II) in a mineral (e.g. magnetite) is able to reduce U(VI) to U(IV) and to compare this
354 ability with that of Fe(II) that is sorbed to a mineral surface (e.g. corundum). The total
355 amount of Fe(II) in the used magnetite suspensions is about 0.002 M as estimated
356 according to Missana et al. (2003), who prepared magnetite at the same conditions as in
357 our study. Measured Fe(II) concentrations in our magnetite suspensions were around 4.3
358 $*10^{-5}$ ($\pm$ $5*10^{-5}$) M independently of the pH (6-10), which is almost consistent with the
359 low solubility of magnetite. In contrast, when Fe(II) was added to the corundum solutions
360 (0.001 M), Fe(II) would bind to the mineral surface by sorption or in presence of
361 bicarbonate also precipitate as siderite. The strong variation of the iron concentration is
362 consistent with the pH dependence of the sorption/ precipitation process ($3*10^{-5}$ M and
363 $5*10^{-6}$ M at pH 8 and 10, respectively; Table1).
364 Sorption reactions are controlled by the amount of surface sites and the kind of surface
365 groups of the used minerals. Due to different surface areas of the two minerals used in
366 our study (magnetite: 19.7 m^2/g; corundum: 14.5 m^2/g), we compare in the following
367 surface area normalized uranium removal from the aqueous phase (for suspensions with
368 $3*10^{-5}$ M initial uranium concentration). The amount of surface area normalized uranium
369 removal (at pH 8) is slightly lower for magnetite ($7.6*10^{-7} \pm 3.9*10^{-9}$) compared to
370 corundum ($1.0*10^{-6} \pm 5.1*10^{-9}$ mol/m^2).
371

372 **3.2. Surface analysis by XPS**

373 The solid residues after centrifugation of magnetite and corundum suspensions treated at
374 pH 8 before and after acidification to pH 4 in presence and absence of bicarbonate and

375 Fe(II) were analyzed by XPS. This technique allows not only determining quantitatively
376 the elemental composition of solid surfaces but also their redox state.

377 **Total elemental composition**

378 The elemental composition of the mineral surfaces after reaction with bicarbonate, U(VI),
379 and Fe(II) were measured by XPS. Results are summarized in Table 3. High Na and Cl
380 concentrations (0.2-2.5 atomic-%) result from the use of NaCl as inert electrolyte in all
381 solutions. Occasionally, trace amounts of impurities of P, Si, K where found. The surface
382 carbon content (2.6-8.9 atomic-%) does not correlate with the input of bicarbonate, but
383 derives from impurities of the minerals, solution reagents or from adventitious
384 hydrocarbon. Uranium surface concentration ranges between 0.04 and 0.6 atomic-% and
385 is clearly higher for magnetite compared to Fe(II) containing corundum samples (Table
386 3). This result differs from the surface area normalized uranium concentration as
387 mentioned above, where the opposite effect was observed, but can be explained by the
388 different measurement techniques: While BET measures the sorption of gases on the
389 whole surface area of a sample, XPS acquires elemental intensities on always 1mm^2 of
390 geometric surface while penetrating to a certain depth beneath the surface (e.g around 5
391 nm in case of magnetite). The relatively high surface concentration as observed for the
392 (Fe(II)- and bicarbonate free) corundum suspension (0.6 atomic %; Table 3) suggests that
393 in this case uranium precipitated on the mineral surface (e.g. as schoepite).

394 **Redox state of uranium**

395 XPS analysis were mainly performed to get evidence if U(VI) was removed from the
396 solutions due to reduction by Fe(II) or due to U(VI) sorption or co-precipitation. Mostly,
397 XPS elemental lines shift to lower binding energies with decreasing redox state. When

398 comparing the XPS spectra of corundum with magnetite (Fig. 5 and 6) it becomes
399 obvious that the uranium peaks of corundum samples are much broader and exceed to
400 lower energies than the theoretical value of U 4f for U(IV), which is at 380 eV. This
401 broadening can be explained by lateral differential surface charging of the isolating
402 corundum due to emission of the electrons during the measurement. Therefore, corundum
403 XPS spectra can only be compared to other corundum spectra and not directly to
404 magnetite.
405 The corundum sample which was amended with Fe(II) (Fig. 5, Spectrum b) shows a
406 slight broadening of the U 4f peaks towards lower binding energy values compared to
407 Fe(II)-free corundum indicating a slightly increased amount of reduced uranium (Fig. 5
408 Spectrum a). This reduction was also optically visible by the formation of black
409 precipitates, (which is the color of the mineral uraninite, UO_2), in the otherwise milky-
410 whitish corundum suspension. In contrast, the Fe(II)-free corundum suspensions
411 remained of whitish color during the experiment. In this latter sample, the U(IV) content
412 was determined by XPS to be 11 % of the uranium detected on the surface (Table 3),
413 which might result from the instrument error or from reduction of U(VI) by Fe(II)
414 impurities contained within the corundum as mentioned above. The additional presence
415 of bicarbonate in the corundum suspension strongly increased the amount of reduced
416 uranium species as the stronger shift of the U4f peaks to lower energies demonstrates
417 (Figure 5, Spectrum d). This shift even exceeds the U(IV) elemental line, which could be
418 explained by the presence of an element with lower Pauling's electonegativity than
419 uranium (1.7) to be in the second shell of U(IV) like Na (0.9) or Al (1.5): U(IV)-O-Na or
420 U(IV)-O-Al. However, the discussion of that phenomenon is beyond the scope of this

421 paper. Since the amount of uranium bound to the corundum is very similar in
422 bicarbonate-free and in bicarbonate containing suspensions kept at pH 8 (99.2 to 99.8 %;
423 Table 1), this peak shift strongly indicates that in the presence of bicarbonate more
424 surface bound U(VI) has been reduced than in absence of bicarbonate.
425 A similar shift to lower energies was observed in XPS spectra of magnetite suspensions
426 amended with bicarbonate (Figure 6). The peak positions of carbonate-free treated
427 magnetite samples were between the literature values for U(VI) and U(IV) oxides (U $4f_{7/2}$
428 at 380.8 eV (as UO_2) and 382.4 (as UO_3; Wersin et al., 1994), indicating that both redox
429 states of uranium are present in this sample. The finding of U(IV) in this sample implies
430 that Fe(II) originating from magnetite is able to reduce U(VI) on the mineral surface. The
431 ratio of U(IV) to Fe(tot) as measured by XPS on the mineral surfaces is a measure of the
432 availability of Fe(II) for uranium reduction inasmuch one can assume that the higher this
433 value is, the better available is the Fe(II) (Table 3). The U(IV)/Fe(tot) ratio is quite
434 similar for both minerals (0.004 to 0.01 at pH 8). However, due to different binding
435 forms of Fe(II) in the minerals (structurally and adsorbed, respectively) the U(IV)/Fe
436 ratio should be considered separately for magnetite and corundum. For both minerals the
437 U(IV)/Fe(tot) ratio increases in presence of bicarbonate indicating again better uranium
438 reduction in presence of bicarbonate.
439 XPS spectra were also obtained for pH 4 acidified corundum and magnetite samples
440 (Figure 5 and 6). It was expected that the acidification removes the weakly bound U(VI)
441 species (sorbed or co-precipitated) from the surface, whereas the sparingly soluble UO_2
442 (U(IV)) would remain on the surface. However, experimental results in this line were
443 obtained only for the corundum suspension, where the U(IV) content on the minerals

444 was 100 and 70 % of the total surface bound uranium. However, in bicarbonate-free,
445 Fe(II) containing corundum suspensions, the uranium surface concentration decreased
446 strongly (to 0.04 atomic-%; Table 3) indicating either re-oxidation of U(IV) (this could
447 be possible by Fe(III), which could have been formed as consequence of decreased pH
448 and increased Eh conditions due to acidification) or that most uranium occurs in this
449 sample as U(VI), which is desorbing at low pH. In case of bicarbonate amended
450 corundum suspensions, the surface uranium content remained almost constant (0.1 and
451 0.12 atomic %, respectively) indicating that reduced uranium-carbonate surface
452 complexes are more resistant against acidification. In magnetite samples, the total
453 uranium concentration at the mineral surfaces remained more or less constant during
454 acidification. However, the U(IV) content drastically decreased (to 5 and 12 % in absence
455 and presence of bicarbonate, respectively; Table 3). One possible explanation for this is
456 that the reduced form of uranium is a weakly crystalline phase (e.g. amorphous UO_2 or
457 U_4O_9) which dissolves more easily at low pH. The fact that the solubility of minerals
458 changes in dependence of their crystallinity (the more amorphous a mineral is, the more
459 easily it dissolves) is well known (Schindler et al., 1963) and explains that the freshly
460 formed uraninite dissolves more easily than an aged one. However, since most uranium
461 remains on the mineral surface this explanation is not very likely. The other explanation
462 is, as mentioned for the corundum samples, that Fe(II) oxidises at the low pH value to
463 Fe(III) which in turn oxidizes U(IV) to U(VI) and desorbs from the surface.

464 **Redox state of iron**

465 In our study, iron(II) is the only plausible reducing agent for U(VI). Consequently, the
466 concentration of Fe(III) on the mineral surfaces should increase during reaction, because

467 Fe(III) usually precipitates as an oxide or hydroxide phase at neutral to basic pH
468 conditions. Thus the XPS Fe 2p spectra is expected to shift towards higher energies.
469 However, compared to the bulk iron, the change in Fe(III) surface concentration is too
470 small to cause detectable changes in the spectra. Consequently, the Fe 2p spectra of all
471 but one sample looked almost identically (Fig. 7a). The only exception was the
472 bicarbonate amended magnetite sample: Clearly, the amount of Fe(II) increased in this
473 sample as compared to other samples (Fig. 7a). We suggest from this observation that a
474 secondary Fe(II) phase, presumably siderite ($FeCO_3$), has formed on the magnetite
475 surface. Additional support for siderite formation was obtained, by comparing also the O
476 1s spectra, where also the bicarbonate amended magnetite sample differed from the
477 others: The peak is broadened towards higher binding energies (Fig. 7b), which is typical
478 for a carbonate phase (Heuer and Stubbins, 1999). These observations are consistent with
479 the suggested formation of a secondary Fe(II) carbonate phase on the magnetite surface
480 already discussed in Section 3.1.3. Moreover, when acidifying this sample to pH 4 both,
481 the O 1s and Fe 2p XPS spectra loose their previously described special features,
482 indicating the re-dissolution of siderite.
483 The Fe 2p and O 1s spectra were measured also for the corundum samples containing
484 Fe(II) and carbonate. However, the Fe 2p lines were quite broad thereby not allowing any
485 interpretation of the data.
486

487 **3.3 Uranium reduction processes**

488 This study revealed that Fe(II) that is adsorbed to mineral surfaces (corundum) or
489 structurally bound in a mineral (magnetite) is able to reduce U(VI) to U(IV). This ability

490 is increased in bicarbonate solutions (1 mM). However, the presence of bicarbonate also
491 increased the amount of dissolved uranium in our experiments. The latter effect was also
492 observed by Behrends and van Kapellen (2005), who concluded, consequently, that
493 U(VI) reduction is inhibited in presence of bicarbonate (45 mM). However, from
494 microbiological studies it has also been found that U(VI) is more bio-available for
495 microbial reduction when present as a carbonate complex (Behrends and van Kapellen,
496 2005; Wall and Krumholz, 2006). By means of spectroscopically investigations (XPS),
497 our study gives now for the first time direct evidence that U(VI) reduction is facilitated in
498 diluted bicarbonate solutions. Results obtained within our study indicate two pathways
499 (potentially simultaneously) to be responsible for this effect: (i) in presence of Fe(II), the
500 formation of siderite is very probable, which accumulates on the solid surfaces where it
501 acts as an easily available pool of Fe(II) with the solid surface simultaneously acting as a
502 catalyst for U(VI) reduction. The redox- and pH- conditions of the suspension control the
503 siderite solubility, which dissolves with decreasing pH, simultaneously releasing the
504 previously bound uranium.
505 The other proposed pathway (ii) is independent from the presence of Fe(II) and relates to
506 the reactivity of U(VI): Results from our work in accordance with previous studies in the
507 literature, gave evidence that U(VI) forms (relatively) stable complexes with carbonate
508 anions (e.g. $UO_2(CO_3)_2^{2-}$ or UO_2CO_3), which predominantly remain dissolved as aqueous
509 complexes. However, a considerable fraction of these complexes are also known to sorb
510 to mineral surfaces and evidence of ternary surface complexes has been reported for the
511 surface of hematite by combination of different spectroscopic techniques (Fourier
512 Transform infrared and X-ray absorption fine structure; Ho and Miller, 1985), as well as

513 of measurements of the electrophoretic mobility of hematite-uranium-carbonate particles
514 (Bargar et al., 2000). These studies described the structures of these negatively charged,
515 ternary surface complexes as innersphere, metal bridged (hematite-U(VI)-carbonato)
516 complexes with, depending on the pH, either monomeric or dimeric character (Ho and
517 Miller, 1985, Bargar et al., 2000). We propose that these surface-attached, carbonate
518 complexes can be more easily reduced to U(IV) than uncomplexed U(VI) species.
519 Possibly, the reduction step of U(VI)-carbonate- complexes goes via an U(IV) carbonate
520 species. The existence of U(IV) carbonate complexes ($U(CO_3)_4^{4-}$ and $U(CO_3)_5^{6-}$) was
521 described by Bruno et al. (1989), who also found small amounts of U(IV) in natural
522 waters to be bound in such complexes, which supports our second pathway for mediation
523 of U(VI) reduction by bicarbonate.
524 For our experiments in the bicarbonate system one can assume that dissolved U(VI)
525 formed first aqueous, carbonate complexes. Partially they sorbed to the mineral surfaces,
526 where the Fe(II) reduced the U(VI) carbonates to U(IV) carbonates. In natural systems, it
527 can be expected that over long time, these U(IV) carbonates age to form more stable
528 uranium oxides, which are in the beginning less crystalline and more soluble, until finally
529 the well-crystalline minerals UO_2 and U_3O_8 form. This hypothesis is supported by our
530 observation of the stability of the uranium surface complexes due to acidification: The
531 uranium release from the mineral surfaces was strongest in the corundum suspension
532 (with no iron and bicarbonate), where solely uranyl was expected to bind to the surface.
533 Next strongest was the uranium release in corundum suspensions containing Fe(II) and
534 bicarbonate, followed by magnetite with bicarbonate (the latter both would contain U(IV)

carbonate complexes) and finally by bicarbonate-free magnetite, where consequently hardly soluble UO_2 precipitation could be expected.

To summarize, within this study we found evidence on the catalyzing effect of dilute bicarbonate solutions on the reduction of U(VI) by Fe(II). These results elucidate the role of carbonate ubiquitously present in groundwater on the migration of uranium.

Acknowledgments

This research was supported by the European research project FUNMIG and the network of Excellence for Actinide Sciences (ACTINET project 05-13). The authors would like to thank Peter Kunze, student apprentice at the FZK for his effort adjusting the pH values and the FZK-INE ICP laboratory.

551 **References**

552 Baborowski, M., Bozau, E., 2006. Impact of former mining activities on the uranium
553 distribution in the River Saale (Germany). Applied Geochemsitry 21(6), 1073-1082.
554 Bargar, J. R., Reitmeyer, R., Lenhart, J.J., Davis, J.A., 2000. Characterization of U(VI)-
555 carbonato ternary complexes on hematite: EXAFS and electrophoretic mobility
556 measurements. Geochim. Cosmochim. Acta 64 (16), 2737-2749.
557 Behrends, T., van Kapellen, P. (2005). Competition between enzymatic and abiotic
558 reduction of uranium(VI) under iron reducing conditions. Chemical Geology 220 (3-
559 4), 315-327.
560 Blatt, H., Tracy, R.J., 1996. Petrology, 2nd edition, New York: Freeman, 66.
561 Bruno, J., Grenthe, I., Robouch, P., 1989. Studies of metal carbonate equilibria 20.
562 Formation of tetra(carbonato)uranium(IV) ion, $U(CO_3)_4^{4-}$, in hydrogen carbonate
563 solutions. Inorganica Chimica Acta 158 (2), 221-226.
564 Burns, P.C. 2005. U6+ minerals and inorganic compounds: Insights into an expanded
565 structural hierarchy of crystal structures. Canadian Mineralogist 43, 1839-1894.
566 Cornell, R.M., Schwertmann, U., 1996. The iron oxides. VCH Weinheim.
567 Duff, M. C., Coughlin, J. U. Hunter, D. B., 2002. Uranium co-precipitation with iron
568 oxide minerals. Geochim. Cosmochim. Acta, 66, 3533-3547.
569 Felmy, A.R., Rai, D., Schramke, J.A., Ryan, J.L., 1989. The solubility of plutonium
570 hydroxide in dilute-solution and in high-ionic-strength chloride brines. Radiochimica
571 Acta, 48(1-2), 29-35.
572 Grenthe, I., Ferri, D., Salvatore, F., Riccio, G., 1984. Studies on metal carbonate
573 equilibria 10. A solubility study of the complex-formation in the uranium(VI) water

carbon-dioxide (G) system at 25 degrees. C. Journal of the Chemical Society-Dalton Transactions, 11, 2439-2443.

Heuer, J.K., Stubbins, J.F., 1999. An XPS characterization of $FeCO_3$ films from CO_2 corrosion. Corrosion Science 41 (7), 1231-1243.

Ho, C. H., Miller, N. H., 1985. Effect of humic acid on uranium uptake by hematite particles. J. Colloid and Interface Sci.106 (2), 281-288.

Ho, C. H., Miller, N. H., 1986. Adsorption of uranyl species from bicarbonate solutions onto hematite particles. J. Colloid and Interface Sci. 110, 165-171.

Ilton. E. S., Haiduc, A., Moses, C. O., Heald, S.M., Elbert, D.C., Veblen, D.R., 2004. Heterogeneous reduction of uranyl by micas: Crystal chemical and solution controls. Geochim. Cosmochim. Acta, 68(11), 2417-2435.

Ilton, E. S., Heald, S. M., Smith, S. C., Elbert, D., Liu, C., 2006. Reduction of uranyl in the interlayer region of low iron micas under anoxic and aerobic conditions. Environ. Sci. Technol., 40 (16), 5003 -5009.

Jeon, B.H., Dempsey, B.A., Burgos, W.D., Barnett, M.O., Roden, E.E., 2005. Chemical reduction of U(VI) by Fe(II) at the solid-water interface using natural and synthetic Fe(III) oxides. Environ. Sci. Technol., 39 (15), 5642-5649.

Langmuir, D., 1978. Uranium solution-mineral equilibria at low temperatures with applications to sedimentary ore-deposits. Geochim. Cosmochim. Acta, 42 (6), 547-569.

Metz, V., Kienzler, B., Schüßler, W., 2003. Geochemical evaluation of different groundwater–host rock systems for radioactive waste disposal. Journal of Contaminant Hydrology 61 (1-4), 265-279; 8th International conference on chemistry

597 and migration behavior of actinides and fission products in the geosphere - Migration
598 01.
599 Missana, T., Maffiotteb, C., García-Gutiérreza, M., 2003. Surface reactions kinetics
600 between nanocrystalline magnetite and uranyl. Journal of Colloid and Interface
601 Science 261 (1), 154-160.
602 Missana, M. Garcia-Gutierrez, Fernndez, V., 2003. Uranium(VI) sorption on colloidal
603 magnetite under anoxic environment: experimental study and surface complexation
604 modelling. Geochim. Cosmochim. Acta, 67, 2543-2550.
605 Mustafa,S., Dilara, B., Neelofer, Z., Naeem, A., Tasleem, S. 1998. Temperature effect on
606 the surface charge properties of γ-Al_2O_3 J. Colloid and Interface Sci. 204, 284–293.
607 Nguyentrung, C., Begun, G. M., Palmer, D. A., 1992. Aqueous uranium complexes 2.
608 Raman-spectroscopic study of the complex-formation of the dioxouranium(VI) ion
609 with a variety of inorganic and organic ligands. Inorganic Chemistry 31 (25), 5280-
610 5287.
611 Payne, R. B., Gentry, D. M., Rapp-Giles, B. J., Casalot, L., Wall, J. D., 2002. Uranium
612 reduction by desulfovibrio desulfuricans strain G20 and a cytochrome c3 mutant.
613 Appl. Environ. Microbiol., 68(6), 3129–3132.
614 Privalov, T., Schimmelpfennig, B., Wahlgren, U., Grenthe I., 2003. Reduction of
615 uranyl(VI) by iron(II) in solutions: An ab initio study. J.of Physical Chemistry A 107
616 (4), 587-592.
617 Puigdomenech, I., 2004. HYDRA and MEDUSA chemical equilibrium software.
618 Software and documentation available from http://web.telia.com/~u15651596/.

619 Rai, D., Gorby, Y. A; Fredrickson, J. K., Moore, D. A., Yui, M. 2002. Reductive
620 dissolution of PuO_2(am): The effect of Fe(II) and hydroquinone. Journal of Solution
621 Chemistry, 31, 433-453.
622 Rovira, M., El Aamrani, S., Duro, L., Giménez, J., de Pablo, J., Bruno, J., 2007.
623 Interaction of uranium with in situ anoxically generated magnetite on steel. J. Haz.
624 Materials, 147, 726 -731.
625 Schindler, P., Michaelis, W., Feitknecht, W., 1963. Die Löslichkeit gealterter Eisen(III)-
626 hydroxid-Fällungen. Helvetica Chimica Acta 46, 444-449.
627 Scott, T. B., Allen, G. C., Heard, P. J., Randell, M. G., 2005. Reduction of U(VI) to
628 U(IV) on the surface of magnetite. Geochim. Cosmochim. Acta, 69 (24), 5639-5646.
629 Seah, M.P., Gilmore, I.S. Beamson, G., 1998. XPS: Binding energy calibration of
630 electron spectrometers 5 - Re-evaluation of the reference energies. Surf. Interface
631 Anal. 26, 642-649.
632 Wall, J. D., Krumholz, L., 2006. Uranium reduction. Annu. Rev. Microbiol. 60,149–66.
633 Wersin, P., Hochella, M. F., Persson, P., Redden, G., Leckie, J. O., Harris, D. W., 1994.
634 Interaction between aqueous uranium(VI) and sulfide minerals – spectroscopic
635 evidence for sorption and reduction. Geochim. Cosmochim. Acta, 58 (13), 2829-
636 2843.
637 WHO, 2004. Uranium in drinking water. Chemical fact sheets of WHO guidelines for
638 Drinking-water quality, 3rd edition.
639 Zhou, P., Gu, B., 2005. Extraction of oxidized and reduced forms of uranium from
640 contaminated soils: Effects of carbonate concentration and pH. Environ. Sci.Technol.,
641 39 (12), 4435 -4440.

Figure captions

Figure1a. Predominance diagram for uranium-mineral suspensions in 10 mM NaCl as calculated with Hydra/Medusa software (Puigdomenech, 2004). Data points represent measured values of pH and uranium concentration in different magnetite suspensions. Initial values (open symbols) are at pH 6, 8, 10 and at uranium concentration of $2.9*10^{-5}$ M (triangles), $8.9*10^{-6}$ M (diamonds) and $9.9*10^{-8}$ M (squares). Filled symbols represent final measured data.

Figure1b. Predominance diagram for uranium-mineral suspensions containing 10 mM NaCl and 1 mM CO_3^{2-} as calculated with Hydra/Medusa software (Puigdomenech, 2004). Data points are measured values of pH and uranium concentration. Initial data (crosses) are at pH 6, 8, 10 and at uranium concentration of $2.9*10^{-5}$ M. Filled symbols represent final concentration of uranium in corundum-Fe(II) amended suspensions (squares) and in magnetite suspensions (triangles).

Figure 2a. Eh/pH diagram for the iron equilibrium system. Open diamonds represent corundum and black diamonds represent magnetite suspensions. Long-dashed lines give the stability line of H_2 and O_2, respectively. The short-dashed line shows the equilibrium area of a solid Fe(II)-/Fe(III) buffer (Felmy et al., 1989; Rai et al., 2002). Other lines represent predominance areas of Fe(II) and Fe(III) species as calculated with Hydra/Medusa software with 1 mM CO_3^{2-} and a 0.01 mM Fe concentration. ("c" in the diagram indicates a solid phase.)

Figure 2b. Predominance diagram for Fe(II) species in a carbonate solution (1 mM). Data points represent measured iron concentrations and pH values of solutions reacted with corundum (open diamonds) and magnetite (black diamonds).

Figure 3. Uranium concentration in solutions containing magnetite, magnetite amended with 1 mM HCO_3^-, corundum amended with 1 mM Fe(II) and corundum amended with each 1 mM Fe(II) and HCO_3^-, measured after the experiment at pH 8 (Table 1 and 2 indicate the final pH values) and after re-acidification to pH 4. Initial uranium concentration was $2.95*10^{-5}$ M.

Figure 4. Uranium concentration in solutions containing magnetite, magnetite amended with 1 mM HCO_3, corundum amended with 1 mM Fe(II) and corundum amended with Fe(II) and HCO_3^- (each 1 mM), measured after the experiment at pH 8 and 10. Values above the columns indicate final pH values.

Figure 5: XPS uranium 4f spectra on the surface of Al_2O_3 at various conditions:
a) Corundum reacted with U(VI) at pH 8
b) Corundum reacted with U(VI) at pH 8 in presence of 1 mM Fe(II)
c) Sample b) which was later acidified to pH 4
d) Corundum reacted with U(VI) at pH 8 in presence of each 1 mM HCO_3^- and Fe(II).
e) Sample d) which was later acidified to pH 4

The dashed lines indicate the reference binding energies of U $4f_{7/2}$ for U(IV) in UO_2 and U(VI) in UO_3, respectively.

Figure 6: XPS uranium 4f spectra on the surface of Fe_3O_4 at various conditions:
a) Magnetite reacted with U(VI) at pH 8
b) Sample a) which was later acidified to pH 4
c) Magnetite reacted with U(VI) at pH 8 in presence of 1 mM HCO_3^-
d) Sample c) which was later acidified to pH 4

The dashed lines indicate the reference binding energies of U $4f_{7/2}$ for U(IV) in UO_2 and U(VI) in UO_3, respectively.

Figure 7a: XPS Fe 2p spectra on the surface of Fe_3O_4 at various conditions:
a) Magnetite reacted with U(VI) at pH 8
b) Sample a) which was later acidified to pH 4
c) Magnetite reacted with U(VI) at pH 8 in presence of 1 mM HCO_3^-
d) Sample c) which was later acidified to pH 4

The dashed line indicates the reference binding energy of Fe $2p_{3/2}$ for Fe(III) and Fe(II).

Figure 7b: XPS O 1s spectra on the surface of Fe_3O_4 at various conditions:
a) Magnetite reacted with U(VI) at pH 8
b) Sample a) which was later acidified to pH 4
c) Magnetite reacted with U(VI) at pH 8 in presence of 1 mM HCO_3^-
d) Sample c) which was later acidified to pH 4

Positions of oxygen in oxides, water, carbonate and hydroxide are marked.

Tables

Table 1. Chemical properties of different mineral suspensions before (initial) and after (final) the reaction with U(VI) solution over 27 days. Background electrolyte of all solutions was 10 mM NaCl.

Solid phase	$NaHCO_3$ initial (M)	$FeCl_2$ initial (M)	U initial (M)	U final (M)	U removed (%)	pH initial	pH final	E_{h_final} (mV)	Fe(tot) final (M)
Fe_3O_4	-	-	$2.95x10^{-5}$	$2.58x10^{-7}$	99.12	6	7.95	-193	$1.81x10^{-5}$
	-	-	$2.96x10^{-5}$	$1.24x10^{-7}$	99.58	8	8.72	-247	$2.27x10^{-5}$
	-	-	$2.95x10^{-5}$	$4.04x10^{-7}$	98.63	10	10.1	-385	$3.12x10^{-5}$
	-	-	$8.94x10^{-6}$	$2.24x10^{-7}$	97.49	6	8.78	-173	$2.96x10^{-5}$
	-	-	$8.91x10^{-6}$	$1.08x10^{-7}$	98.79	8	8.63	-211	$2.09x10^{-5}$
	-	-	$8.93x10^{-6}$	$2.63x10^{-7}$	97.05	10	9.77	-355	$1.20x10^{-5}$
	-	-	$9.96x10^{-8}$	$3.22x10^{-9}$	96.76	6	8.91	-208	$4.22x10^{-5}$
	-	-	$9.95x10^{-8}$	$2.19x10^{-9}$	97.80	8	8.55	-320	$4.69x10^{-5}$
	-	-	$9.94x10^{-8}$	$1.52x10^{-8}$	84.66	10	9.66	-416	$1.99x10^{-4}$
	$1x10^{-3}$	-	$2.94x10^{-5}$	$7.04x10^{-7}$	97.61	6	8.1	-117	$7.40x10^{-5}$
	$1x10^{-3}$	-	$2.96x10^{-5}$	$2.32x10^{-6}$	92.15	8	8.2	-197	$9.40x10^{-6}$
	$1x10^{-3}$	-	$2.96x10^{-5}$	$1.23x10^{-5}$	58.56	10	10.2	-362	$7.80x10^{-6}$
Al_2O_3	-	$1x10^{-3}$	$2.91x10^{-5}$	$4.35x10^{-6}$ *	85.04	6	6.14	-84	nm
	-	$1x10^{-3}$	$2.88x10^{-5}$	$2.23x10^{-8}$ *	99.92	8	8.1	-143	$3.00x10^{-5}$
	-	$1x10^{-3}$	$2.58x10^{-5}$	$1.48x10^{-8}$ *	99.94	10	10.53	-403	$5.03x10^{-6}$
	-	-	$2.80x10^{-5}$	$1.87x10^{-7}$	99.33	6	8.85	-291	$6.21 x10^{-6}$
	-	-	$2.80x10^{-5}$	$2.88x10^{-7}$	98.97	8	9.32	-208	$2.57 x10^{-6}$
	-	-	$2.94x10^{-5}$	$2.53x10^{-7}$	99.14	10	10.49	-412	$3.55 x10^{-6}$
	$1x10^{-3}$	$1x10^{-3}$	$2.89x10^{-5}$	$2.44x10^{-8}$ *	99.92	6	7.43	-201	$3.70x10^{-4}$
	$1x10^{-3}$	$1x10^{-3}$	$2.84x10^{-5}$	$3.43x10^{-8}$ *	99.88	8	8.45	-265	$3.15x10^{-6}$
	$1x10^{-3}$	$1x10^{-3}$	$2.65x10^{-5}$	$6.65x10^{-8}$ *	99.75	10	10.46	-414	$5.60x10^{-6}$

nm = not measured

*observation: color change (from white to black) in the end of the experiment

Table 2. Chemical properties of different mineral suspensions originally adjusted to pH 8 with highest initial uranium concentration ($2.8*10^{-5}$ - $2.9*10^{-5}$ M; Table 1) measured 48 h after acidification to pH 4.

mineral	$NaHCO_3$ (M)	$FeCl_2$ (M)	U (M)	Fe(II) (M)	pH
Fe_3O_4	-	-	2.81E-6	7.79E-5	3.95
	x	-	1.32E-5	9.46E-5	3.93
Al_2O_3	-	x	1.01E-5	1.95E-4	3.78
	-	-	1.65E-5	-	3.95
	x	x	4.99E-6	1.14E-4	4.12

x : compound was added initially
- : compound was not added

Table 3. Elements determined by XPS (in atomic %) in different samples. Initially, $2.95*10^{-5}$ M U(VI) was added to all samples. Relative atomic concentration results are typically within 10-20 % error. Hydrogen is not measured by XPS.

sample	Al	Fe	O	C	Na	Cl	U	U(IV)/ Fe	U(IV) (%U_{tot})
Al_2O_3 [*1,3]	32.87	---	57.83	5.55	2.00	0.64	0.61	---	11
Al_2O_3 + Fe(II)	30.74	4.52	58.73	4.00	1.04	0.80	0.17	0.012	37
Al_2O_3 + Fe(II); pH 4	26.55	8.92	57.71	4.56	1.41	0.81	0.04	0.004	100
Al_2O_3 + Fe(II)+ HCO_3^-	28.01	4.21	56.93	7.45	2.29	1.01	0.10	0.009	36[*4]
Al_2O_3 + Fe(II)+ HCO_3^-; pH 4	24.37	10.88	56.79	5.88	1.21	0.75	0.12	0.008	70
Fe_3O_4	1.17	37.73	54.01	5.50	1.02	0.25	0.32	0.004	52
Fe_3O_4; pH 4 [*2]	---	33.62	52.95	8.93	2.44	1.04	0.36	0.001	5
Fe_3O_4, + HCO_3^- [*1]	5.91	30.42	57.48	2.60	2.14	0.97	0.33	0.007	68
Fe_3O_4, + HCO_3^-; pH 4 [*3]	---	36.62	51.18	8.18	2.49	1.06	0.21	0.001	12

[*1] traces of potassium (< 0.15 atomic %)
[*2] traces of phosphorous (<0.66 atomic-%)
[*3] traces of silica (<0.4 atomic-%)
[*4] potential occurrence of uranium species of lower redox state than U(IV)

Figure 1a

Click here to download high resolution image

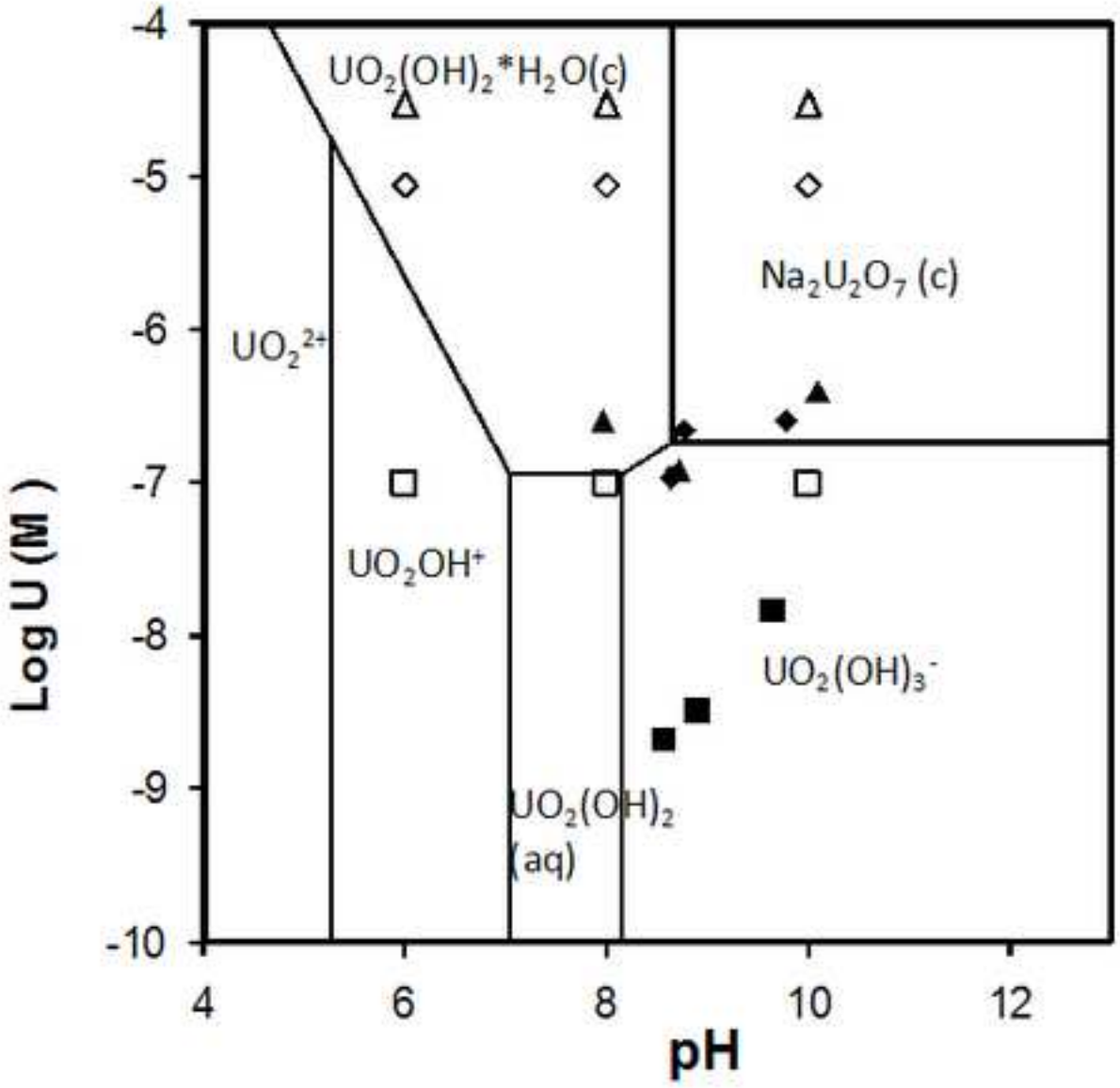

Figure 1b

Click here to download high resolution image

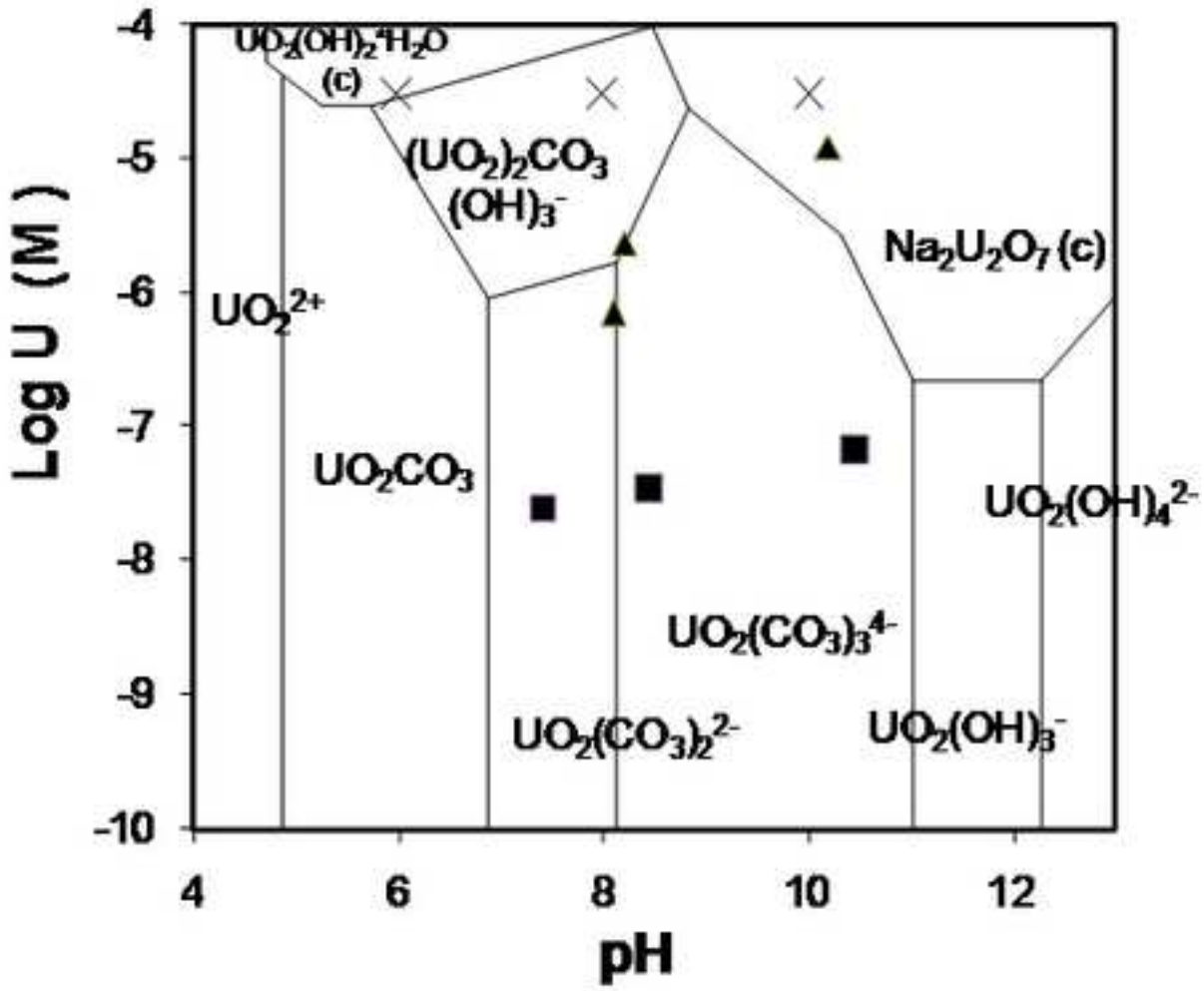

Figure 2a

Click here to download high resolution image

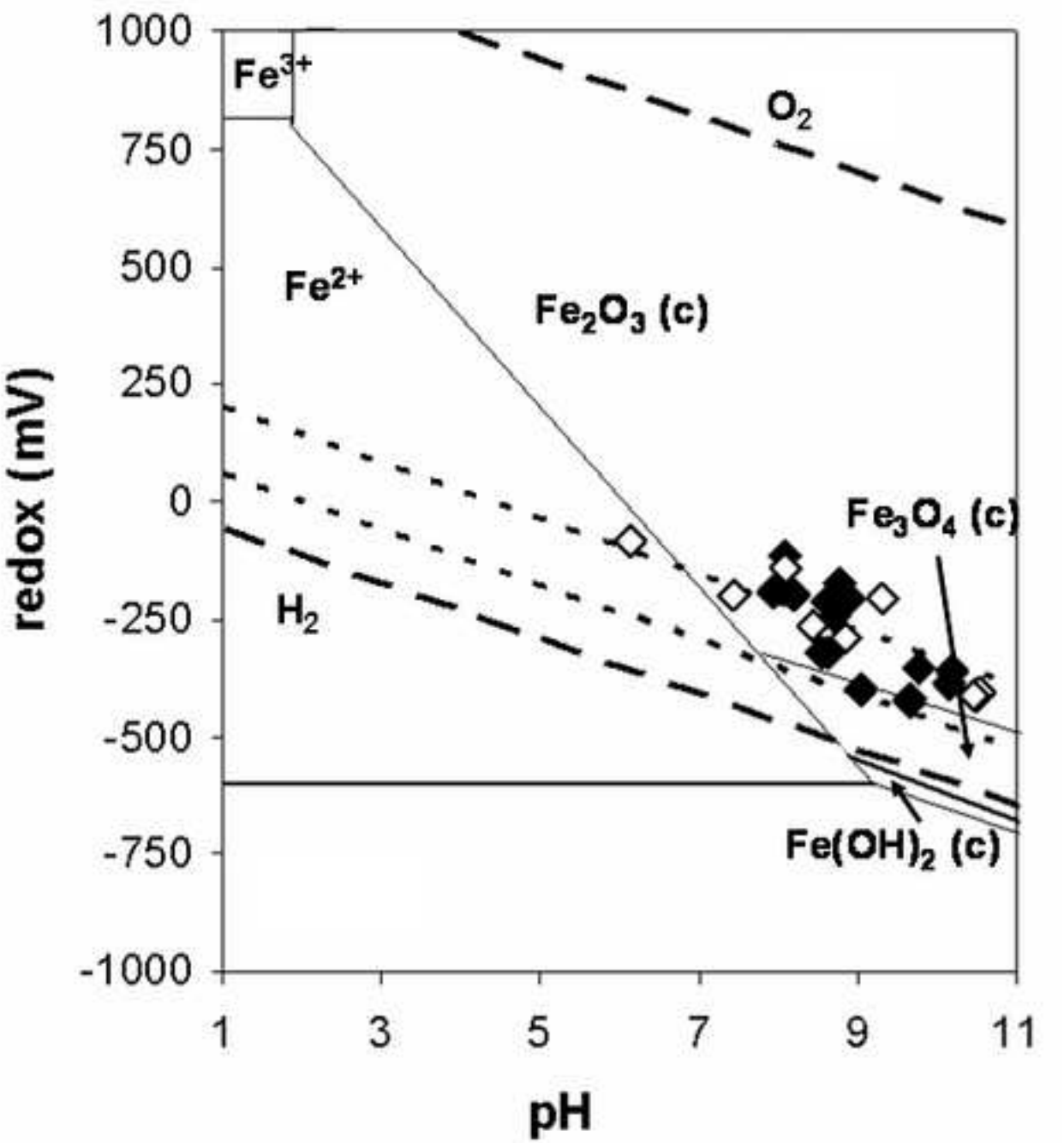

Figure 2b

Click here to download high resolution image

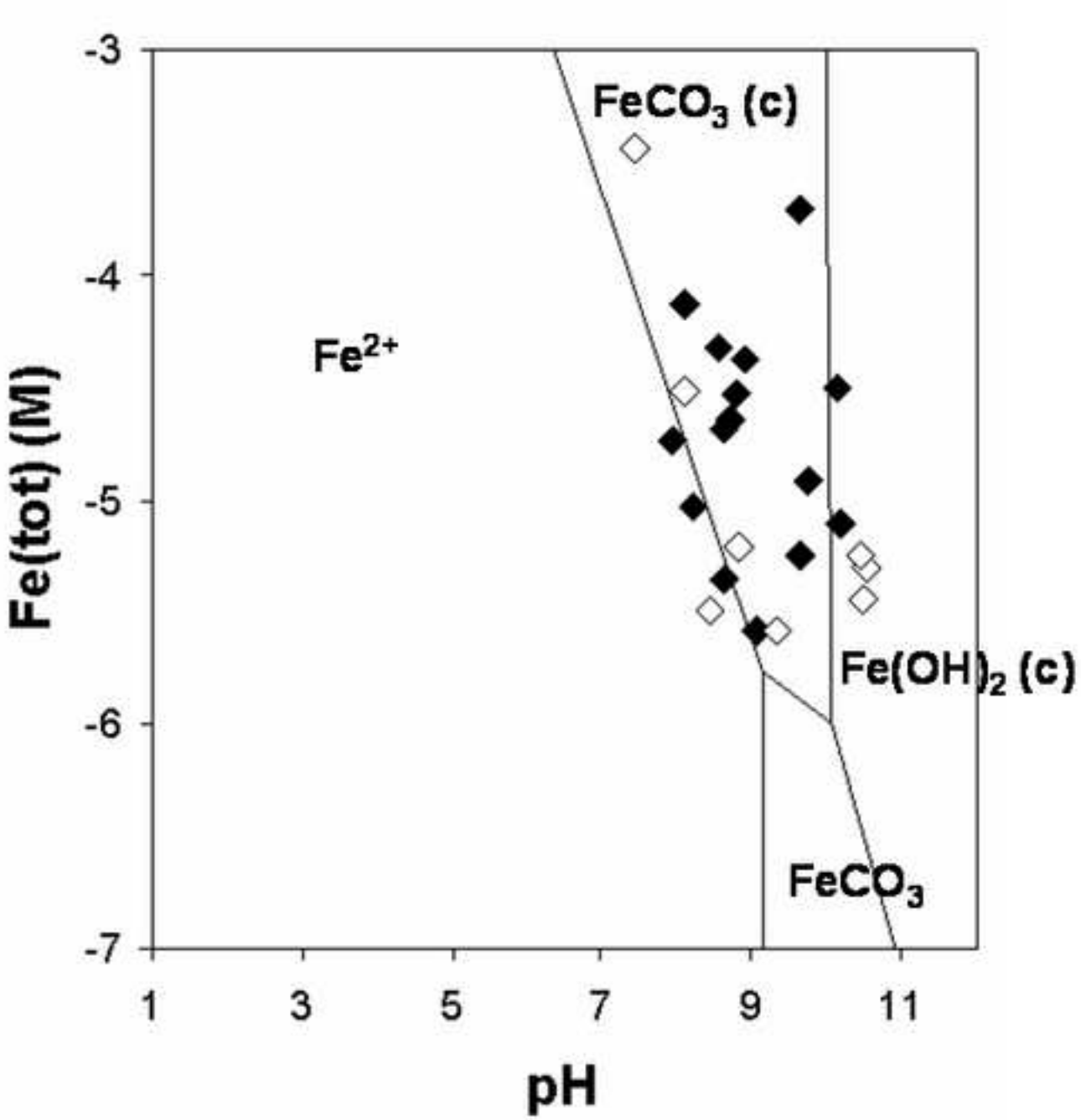

Figure 3

Click here to download high resolution image

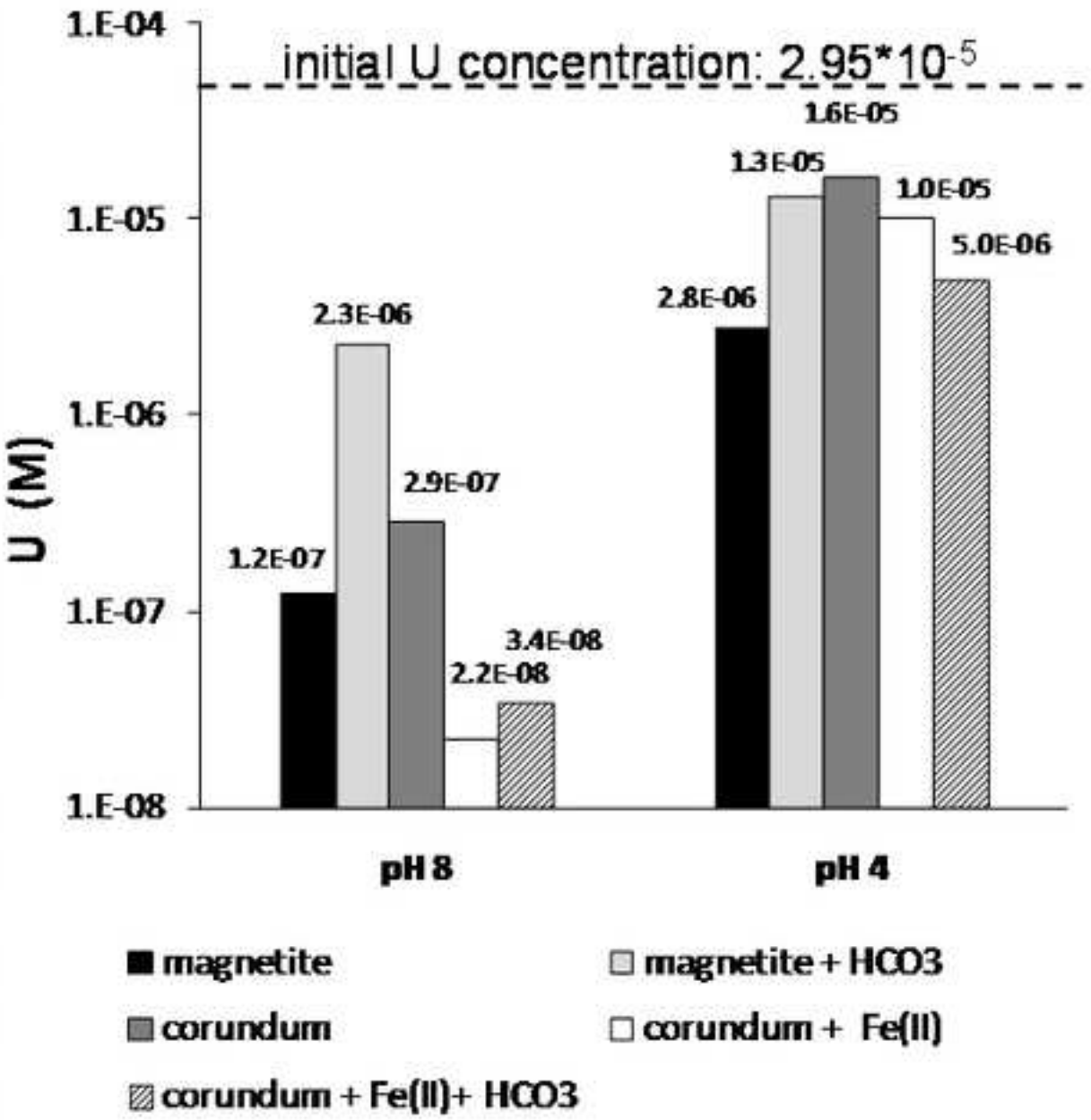

Figure 4

Click here to download high resolution image

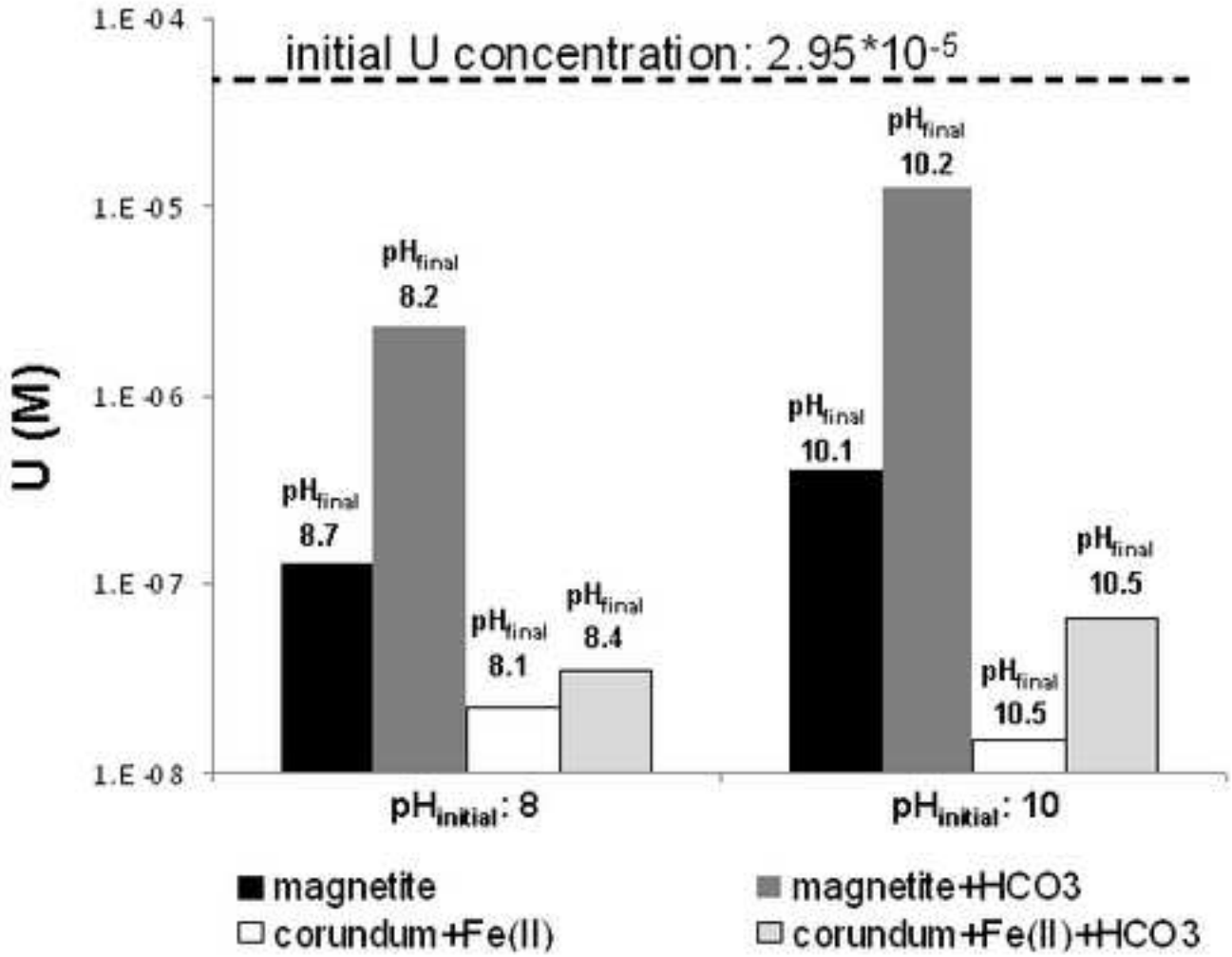

Figure 5

Click here to download high resolution image

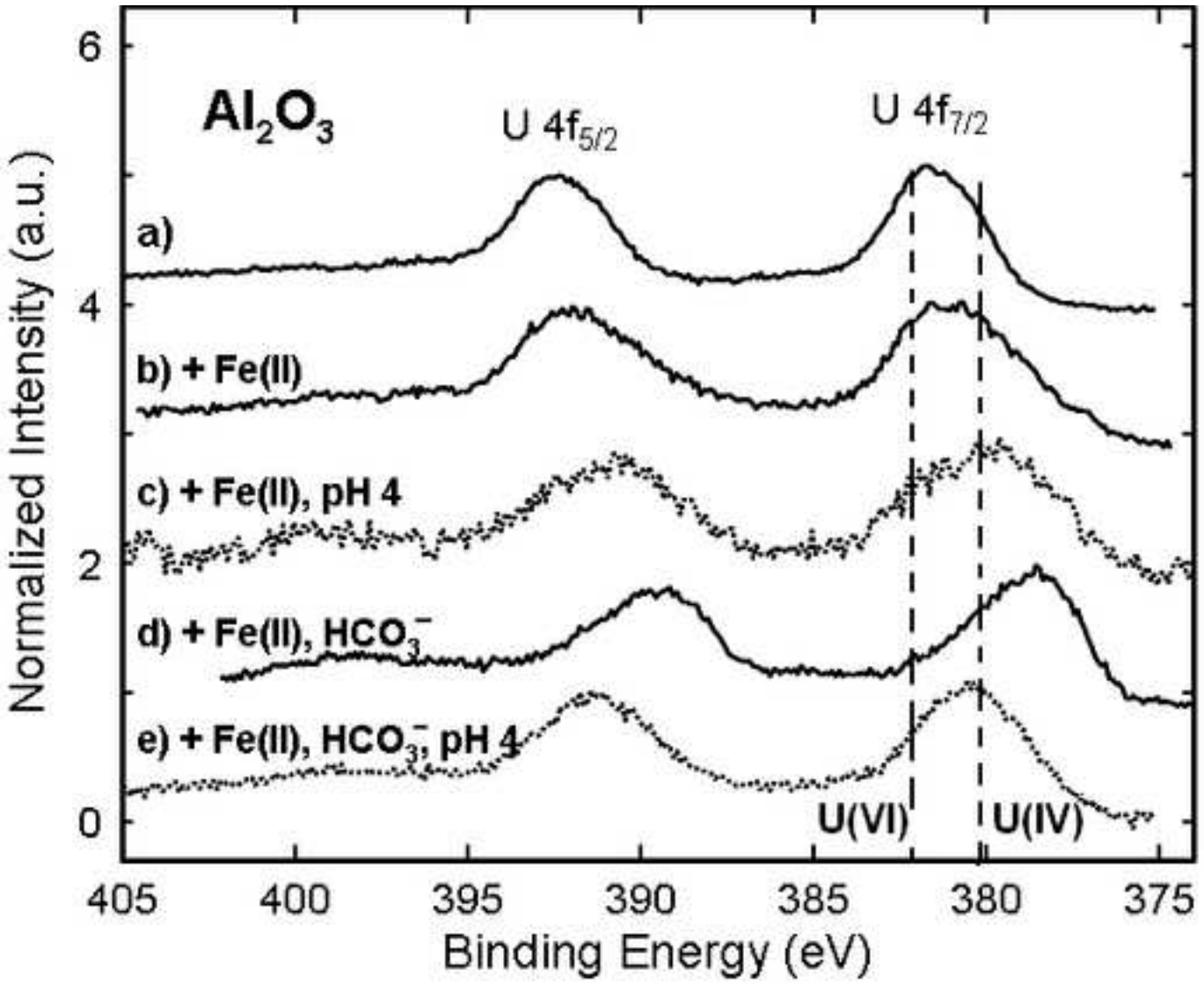

Figure 6

Click here to download high resolution image

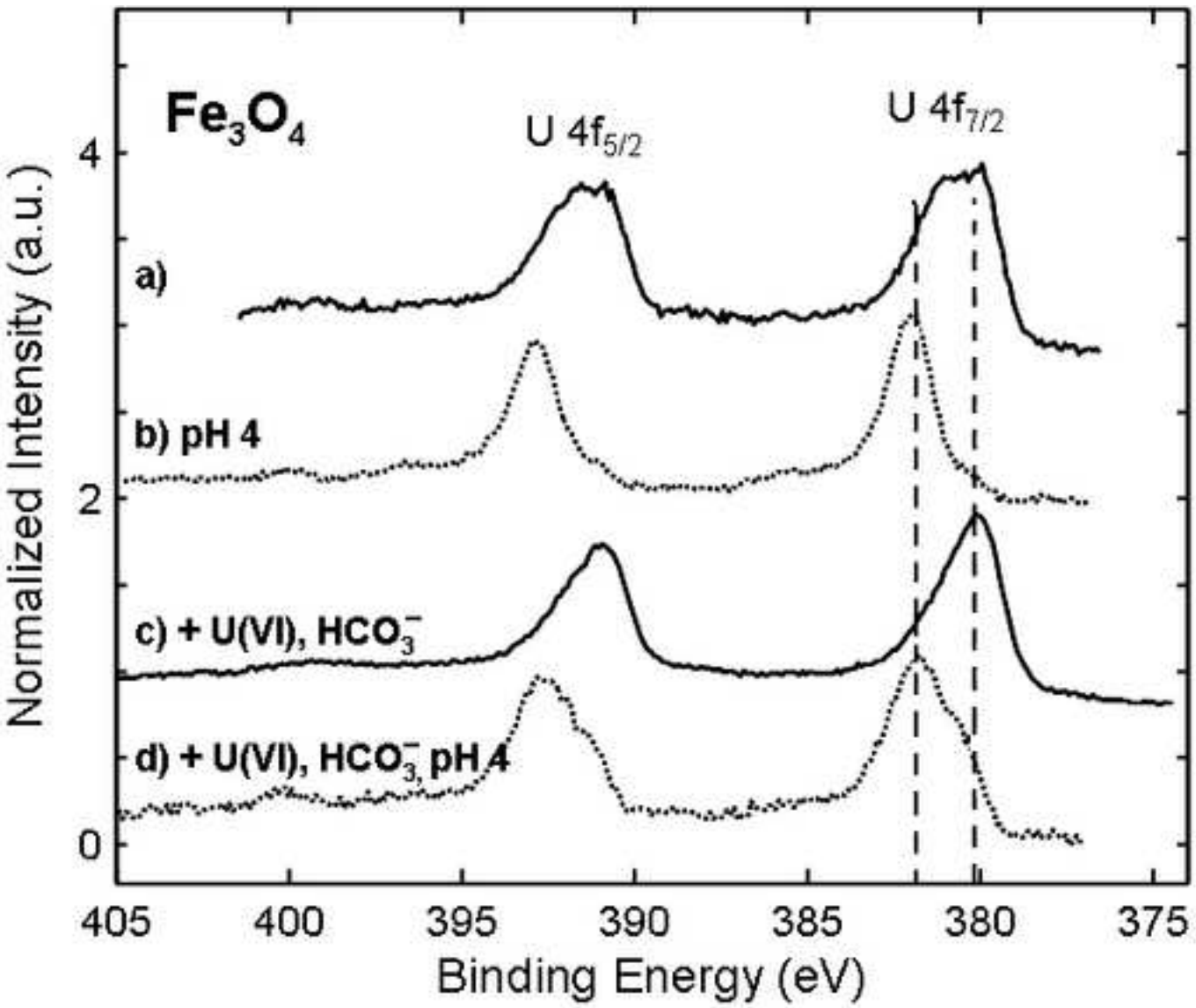

Figure 7a

Click here to download high resolution image

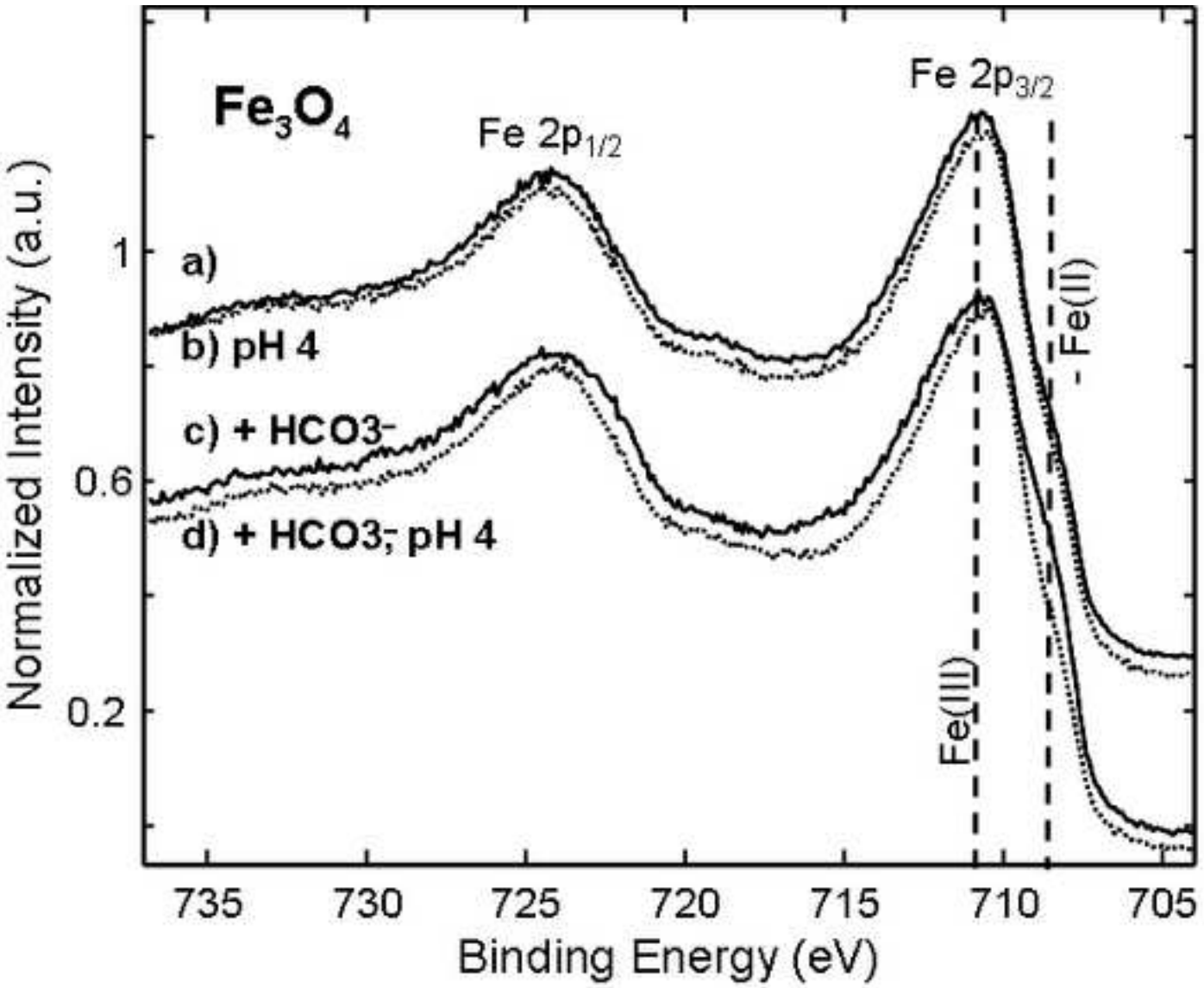

Figure 7b

Click here to download high resolution image